

AD-A093 268

IBM THOMAS J WATSON RESEARCH CENTER YORKTOWN HEIGHTS NY F/6 7/3  
THE VIBRATIONS AND STRUCTURE OF PYRIDINE CHEMISORBED ON A6(111)--ETC(U)  
NOV 80 J E DEMUTH, K CHRISTMANN, P N SANDA N00014-77-C-0366

UNCLASSIFIED

TR-11

NL

1 1 1  
2 3 4  
5 6 7 8 9 10 11 12 13 14 15 16 17 18 19 20 21 22 23 24 25 26 27 28 29 30 31 32 33 34 35 36 37 38 39 40 41 42 43 44 45 46 47 48 49 50 51 52 53 54 55 56 57 58 59 60 61 62 63 64 65 66 67 68 69 70 71 72 73 74 75 76 77 78 79 80 81 82 83 84 85 86 87 88 89 90 91 92 93 94 95 96 97 98 99 100

END  
DATE  
FILMED  
1-8  
DTIC

AD A093268

LEVEL

OFFICE OF NAVAL RESEARCH

Contract N00014-77-C-0366

Task No. NR 056-123

TECHNICAL REPORT NO.11

12

The Vibrations and Structure of Pyridine Chemisorbed on Ag(111):  
the Occurrence of a Compressional Phase Transformation

by  
J.E. Demuth, K. Christmann  
and P. N. Sanda

Prepared for Publication  
in  
Chemical Physics Letters

IBM T.J. Watson Research Center  
Yorktown Heights, NY 10598

November 21, 1980

COPIES  
COLLECTED  
DEC 22 1980  
C

Reproduction in whole or in part is permitted for  
any purpose of the United States Government

This document has been approved for public release  
and sale; its distribution is unlimited

DDC FILE COPY

80 12 22 100

UNCLASSIFIED

SECURITY CLASSIFICATION OF THIS PAGE (When Data Entered)

REPORT DOCUMENTATION PAGE		READ INSTRUCTIONS BEFORE COMPLETING FORM
1. REPORT NUMBER Technical Report, No. 11'	2. GOVT ACCESSION NO. AD-A093	3. RECIPIENT'S CATALOG NUMBER 168
4. TITLE (and Subtitle) The Vibrations and Structure of Pyridine Chemisorbed on Ag(111): the Occurrence of a Compressional Phase Transformation.		5. TYPE OF REPORT & PERIOD COVERED
7. AUTHOR(S) J.E. Demuth, K. Christmann, and P.N. Sanda		6. PERFORMING ORG. REPORT NUMBER
9. PERFORMING ORGANIZATION NAME AND ADDRESS IBM T.J. Watson Research Center, P.O. Box 218, Yorktown Heights, NY 10598		8. CONTRACT OR GRANT NUMBER(s) N00014-77-C-0366
11. CONTROLLING OFFICE NAME AND ADDRESS Office of Naval Research Chemistry Program Office Arlington, VA 22217		10. PROGRAM ELEMENT, PROJECT, TASK AREA & WORK UNIT NUMBERS 11/21 Nov 80
14. MONITORING AGENCY NAME & ADDRESS (if different from Controlling Office) 11/21-2		12. REPORT DATE November 21, 1980
		13. NUMBER OF PAGES
		15. SECURITY CLASS. (of this report) Unclassified
		15a. DECLASSIFICATION/DOWNGRADING SCHEDULE
16. DISTRIBUTION STATEMENT (of this Report)  Approved for Public Release; Distribution Unlimited.		
17. DISTRIBUTION STATEMENT (of the abstract entered in Block 20, if different from Report)		
18. SUPPLEMENTARY NOTES  To appear in Chemical Physics Letters		
19. KEY WORDS (Continue on reverse side if necessary and identify by block number)  Surface, Chemisorption, Vibrations, structure, Pyridine, Bonding, Compressional phase transformation, Silver		
20. ABSTRACT (Continue on reverse side if necessary and identify by block number) High resolution electron energy loss and UV photoemission spectroscopies have been used to study the chemisorption of pyridine on clean Ag(111) at T~140K. Pyridine is weakly chemisorbed and undergoes a compressional phase transformation from a $\pi$ -bonded species to a more weakly bound, nitrogen-lone-pair bonded species. The molecular orientations of both chemisorbed phases are determined.		

DD FORM 1473  
1 JAN 73

UNCLASSIFIED

SECURITY CLASSIFICATION OF THIS PAGE (When Data Entered)

**The Vibrations and Structure of Pyridine Chemisorbed on Ag(111): the Occurrence of a Compressional Phase Transformation†**

J.E. Demuth, K. Christmann,\* and P.N. Sanda\*\*

IBM T.J. Watson Research Center  
Yorktown Heights, New York 10598

**Abstract:** High resolution electron energy loss and UV photoemission spectroscopies have been used to study the chemisorption of pyridine on clean Ag(111) at  $T \sim 140$  K. Pyridine is weakly chemisorbed and undergoes a compressional phase transformation from a  $\pi$ -bonded species to a more weakly bound, nitrogen-lone-pair bonded species. The molecular orientations of both chemisorbed phases are determined.

Accession For	
NTIS GRA&I	<input checked="" type="checkbox"/>
DTIC TAB	<input type="checkbox"/>
Unannounced	<input type="checkbox"/>
Justification	<input type="checkbox"/>
By _____	
Distribution /	
Availability Codes	
Avail and/or	
Dist	Special
A	

† Supported in part by the U.S Office of Naval Research.

\* Permanent address: Institut für Physikalische Chemie der  
Universität München, W. Germany.

\*\* Affiliated with Cornell University, Ithaca, NY 14850

Here we report high-resolution, electron energy loss (EELS), UV-photoemission (UPS) and thermal desorption spectroscopic (TDS) results for pyridine chemisorbed on a clean Ag(111) surface from which we determine its molecular vibrations as well as its orientation on the surface. We find that pyridine exhibits reversible, weak chemisorption on Ag(111) and is  $\pi$ -bonded for coverages up to  $3 \times 10^{14}$  molecules/cm<sup>2</sup>. Increased coverage leads to a structural phase transformation where nitrogen-lone-pair bonding occurs and the molecule becomes inclined ( $\sim 55^\circ$ ) to the surface and rotated ( $\sim 30^\circ$ ) about the molecular  $C_{2v}$  symmetry axis. This compressed structure is more weakly bound to Ag(111) than the  $\pi$ -bonded phase and saturates at coverages of  $\sim 5 \times 10^{14}$  molecules/cm<sup>2</sup>. Such complex bonding and orientational effects have not been observed in previous studies of adsorbed pyridine [1-3] and are important for understanding the nature of surface enhanced Raman scattering for pyridine on Ag as observed in electrochemical [4] and ultra-high vacuum studies [5].

The experimental measurements were performed in two separate ultra-high vacuum (UHV) systems (pressure  $< 1 \times 10^{-10}$  Torr). The first (turbo-molecular pumped) system described elsewhere [6] allows UPS, low-energy electron diffraction (LEED), Auger (AES) and TDS to be performed while the second (ion- and titanium-sublimator-pumped) system permits EELS and work function change measurements. The electron optics for EELS consists of two sets of 2.5 cm hemispherical deflection analyzers with associated focusing optical elements [7] so as to allow the monochromatization, reflection from a sample (total scattering angle of  $90^\circ$ ) and energy analysis of a well-defined ( $< 0.2$  mm dia.), collimated ( $< 1^\circ$ ), low-energy (2-100 eV) electron beam. For the specular reflection of a 3 eV beam off of Ag(111), we have routinely obtained a total system resolution of 65-75 cm<sup>-1</sup> (8-9 mV) with peak counting rates of  $10^6$  Hz. Although both the monochromator and analyzer are in fixed position, the sample rotation is

arranged so as to enable the observation of specular ( $\theta_{in} = \theta_{out}$ ) as well as off-specular ( $\theta_{in} \neq \theta_{out}$ ) scattering events in the plane of incidence.

The Ag(111) surface was prepared by standard mechanical [6] and chemical polishing [8], then annealed and sputter cleaned as determined by AES. This clean, well-ordered Ag(111) sample was then inserted into the EELS system where further sputter cleaning and annealing was performed. Work-function change measurements performed in both UHV systems as well as EELS spectra served to verify surface cleanliness in the HREEL system. The final clean samples were mirror smooth and showed minimal optical defects or irregularities. All chemisorption experiments in the EELS system were done at temperatures of  $\sim 140\text{K}$  as monitored by a chromel-alumel thermocouple. UPS measurements were performed at temperatures down to  $80\text{ K}$ .

Reagent grade pyridine (99.9%) and  $d_5$ -pyridine (99 atom % D) were used in these experiments. Sample dosing was done via the chamber ambient and directly monitored with an ion gauge. (All exposures cited here are in Langmuires, L ( $1\text{L} \approx 10^6 \text{ Torr-sec}$ ) and have been corrected by a gauge factor of 5.8 [9].) The dosages required to produce both the compressional phase and first physisorbed layers were identical in both UHV systems.

Our results indicate that a structural phase transformation occurs for chemisorbed pyridine on Ag(111) at an exposure of  $\sim 0.5\text{L}$ . In Fig.1 we show the EELS vibrational loss spectra of  $d_5$ -pyridine before (solid line) and after (dotted line) this transition. Here, the relative intensities of the CH deformation modes between  $360\text{-}820\text{ cm}^{-1}$  strongly change, especially when compared to the relative IR-absorbances [10,11] also shown in Fig.1. This transition is more striking for normal pyridine  $\text{C}_5\text{H}_5\text{N}$  as shown in Fig. 2 for the chemisorption regime ( $< 1\text{L}$  exposure). For normal pyridine the

CH deformation modes at  $\sim 600$  and  $700\text{ cm}^{-1}$  are clearly separated. Also, the strong decrease in intensity of the  $\sim 700\text{ cm}^{-1}$  feature above  $0.5\text{ L}$  exposure indicates that at least 93% of the lower coverage phase converts to a new structure. The vibrational frequencies for both phases are identical within our experimental uncertainties of  $\pm 5\text{ cm}^{-1}$ .

In order to obtain structural information from the loss spectra of chemisorbed pyridine on  $\text{Ag}(111)$ , we must assign the observed vibrations. At the onset such an assignment would seem formidable based upon the relatively poor resolution of EELS and the fact that pyridine is of low symmetry and has 27 IR-active modes [12]. Fortunately, we find that we can straight forwardly assign most all the observed vibrational losses since (a) only a fraction of the 27 free-molecule modes have significant dipole scattering cross sections (i.e., IR absorbances [10,11], see Fig.1) and (b) all the vibrations we observe are weakly perturbed ( $\Delta\nu_{\text{avg}} = \pm 6\text{ cm}^{-1}$ ) relative to liquid pyridine. In Table I, we list the observed vibrational losses for normal and deuterated pyridine as well as the vibrations for liquid pyridine with absorbances,  $A$  greater than  $\sim 1\%$  of the largest value [10,11]. The symmetry class and mode number as designated by Long and Thomas [12] are also indicated. Comparisons between normal and deuterated pyridine as well as the corresponding relative intensities help in our identification and assignments. We also interpret the  $700\text{ cm}^{-1}$  loss for low coverages of deuterated pyridine as a combination band of  $\nu_{26}$  and the pyridine-metal-stretching vibration (PM) since  $\nu_{26}$  is very intense and has a symmetry which will allow coupling. The resulting (deuterated) pyridine-metal vibration of  $\sim 175\text{ cm}^{-1}$  is also in agreement with that observed for normal pyridine ( $\sim 200\text{ cm}^{-1}$ ) and observed in other pyridine-metal compounds [13]. Interestingly, we see no evidence for the presence of  $\nu_{25}$ , a rather strong IR mode but which has extremely asymmetric deformation motions. This is true for  $\nu_{17}$  which is also not observed. Finally, we cannot assign

(a) which CH-stretching modes we observe due to our limited resolution, nor (b) the character of the 1220 or 1570  $\text{cm}^{-1}$  losses for normal pyridine. Fortunately, these last ambiguities play no role in our structural analysis.

From our assignments in Table I, the observed coverage-dependent changes in the loss spectra of Fig.2 near  $\sim 0.5$  L are associated with a reduction in the intensity of the out-of-plane CH-deformation modes at  $\sim 400$  and  $705 \text{ cm}^{-1}$  and an increase in the in-plane CH-deformation mode near  $610 \text{ cm}^{-1}$  (and similarly for  $d_5$ -pyridine in Fig.1). By comparing the relative intensities of these in-plane and out-of-plane modes and relating them to the "structurally-averaged" dipole-scattering intensities (i.e., IR-absorbances) of liquid pyridine, we can determine the molecular orientation. Here, we exploit the dipole-scattering mechanism for *specular* electron scattering [14] and assume the surface selection rule that only the normal components of these modes will be observed in EELS [15]. For pyridine inclined at an angle  $\theta$  to the surface, the loss intensities for in-plane ( $I_{in}$ ) and out-of-plane ( $I_{out}$ ) deformation modes are related by

$$\frac{A_{in}}{A_{out}} \tan \theta = \frac{I_{in}}{I_{out}},$$

where A is the IR absorbance and we assume a constant transmission function for our spectrometer [16]. Applying this relation to the out-of-plane deformation modes  $\nu_{26}$  and  $\nu_{27}$  and the in-plane deformation mode  $\nu_{10}$  we determine averaged angles of  $\sim 5 \pm 3^\circ$  at low coverages ( $< 0.4$  L) and  $\sim 57 \pm 3^\circ$  at higher coverages (0.6-0.8 L). For these higher coverages we have assumed that the structural conversion is complete. This assumption turns out to be consistent with the resulting geometry which provides (a) the correct relative saturation coverages of both phases and (b) the proposed intermolecular stabilization mechanism as discussed later. Based upon our UPS results (to be described) as well as other chemical arguments



and results [1,2], this strongly-inclined phase has the nitrogen end of the molecule directed into the surface.

For exposures above 0.5 L we also find another in-plane deformation mode at  $1440\text{ cm}^{-1}$  ( $1305\text{ cm}^{-1}$ ,  $d_5$ -pyridine) which also becomes EELS active. This mode turns out to have net motions almost completely perpendicular to the  $C_{2v}$  symmetry plane of the molecule. Again, considering the surface-selection rule [15], leads us to conclude that the molecule is rotated about the  $C_{2v}$  symmetry axis. Applying the aforementioned intensity analysis to  $\nu_{10}$  and  $\nu_{14}$  gives rotational angles of  $24^\circ$  and  $40^\circ$  for normal and deuterated pyridine, respectively. These rotations also change the determined angles of inclination, but only slightly, to  $53^\circ$  and  $48^\circ$  respectively, since  $\nu_{10}$  has little net motions parallel to the  $C_{2v}$  symmetry axis. This leads us to estimate a rotational angle of  $\sim 30^\circ$  and an inclination angle of  $55^\circ \pm 5^\circ$ , respectively. From our off-specular scattering data, we have also estimated an upper limit for non-dipole scattering which does not significantly alter these values. However, we have excluded the losses at  $\sim 1000$  and  $1570\text{ cm}^{-1}$  for normal pyridine (and the corresponding losses for deuterated pyridine) in our intensity analysis as they appear to have strong contributions from non-dipole scattering [17].

Our UPS spectra ( $h\nu = 21.2\text{ eV}$ ) are also consistent with a coverage-dependent reorientation of pyridine on Ag(111). In Fig.3 we summarize difference spectra obtained in the low and high coverage regimes of chemisorbed pyridine as well as for condensed pyridine and gaseous pyridine [18]. Here, we show only the orbitals which correspond to gas phase ionization potentials of less than 12 eV since the higher-lying ( $\pi_2, \pi_3, n$ ) orbitals of chemisorbed pyridine overlap the Ag(111) d-band emission and cannot be resolved with certainty. The character of the ground-state orbital(s) associated with each ionization level is labeled [19] according to the level ordering [20]. The overall displacement in level positions (dotted

lines in Fig.3) for exposures above 1 L is associated with differences in relaxation and initial state polarization shifts for condensed versus chemisorbed species and indicates that all pyridine below this exposure *must be* chemisorbed [21]. After considering a uniform relaxation shift [21], the ionization levels of condensed and gaseous pyridine are nearly identical whereas chemisorbed pyridine shows differences in the relative positions of the high-lying levels. Namely, the low-coverage phase does not show the  $\pi_1$  level which can be shifted to lower energies for a  $\pi$ -bonded species [21] so as to overlap with the  $\sigma_{cc}, "n"$  and  $\sigma_{cc}$  levels. For higher coverages after the phase transformation, the  $\pi_1$  level is observed and the level having nitrogen-lone-pair character ( $\sigma_{cc}, "n"$ ) is perturbed and shifted to lower binding energies. This level is expected to shift if the high-lying nitrogen-lone-pair orbital becomes involved in bonding [22,23].

In Fig.4a and b, we schematically show the bonding orientation of chemisorbed pyridine at low and high coverages and propose a brief phenomenological description of the phase transformation. At low coverages pyridine bonds through the  $\pi$ -orbitals where an additional interaction of the surface via the nitrogen-lone-pair orbital may account for the small initial inclination. As this  $\pi$ -bonded phase approaches saturation coverage, we find that the sticking coefficient drops to almost half its initial value (as determined from UPS versus exposure data) and retains this value even when condensation occurs. Although we see no LEED patterns for any stage of chemisorption [24], a dramatic increase occurs in the electron reflectivity nearing completion of the  $\pi$ -bonded phase. Such phenomena in EELS is generally observed when well-ordered superstructures form [25,26]. We thus believe that a nearly-ideal close-packed ordered array of  $\pi$ -bonded pyridine occurs; and assuming a close-packed but commensurate pyridine monolayer, we estimate it to have a packing density of  $3 \times 10^{14}$  molecules/cm<sup>2</sup>. Continued exposure allows additional molecules to squeeze

into defects or irregularities in the pyridine overlayer causing adjacent domains of molecules to become inclined. The resulting increased packing density produces more space on the surface and allows for island growth of this compressed structure. From the relative coverages determined by UPS, we estimate a density of  $5 \times 10^{14}$  molecules/cm<sup>2</sup> for this compressed phase prior to condensation. This compressional phase transformation is also reversible, and from thermal desorption results, we estimate that it is  $\sim 2$  kcal/mole less strongly bound to the surface than the  $\pi$ -bonded phase.

Although we find  $\pi$ -bonded pyridine to be more strongly bound to Ag(111) than nitrogen-lone-pair bonded pyridine, the latter becomes preferred in the compressed phase. The loss of binding energy upon reorientation of  $\pi$ -bonded pyridine can be regained from intermolecular interactions. Given the aforementioned relative packing densities and our determined angle of inclination for the compressed phase, an attractive  $\pi_3$ -nitrogen-lone-pair interaction may occur (see Fig.4b). Such an interaction is reasonable since these orbitals are nearly degenerate. This interaction also accounts for the determined molecular rotation since the  $\pi_3$  orbital phasing [19] is such as to allow only one side of the molecule to interact with the nitrogen-lone-pair orbital of an adjacent molecule.

In summary, we present evidence that pyridine  $\pi$ -bonds to the Ag(111) surface until it goes through a compressional phase transformation where it then bonds to the surface via the nitrogen-lone-pair orbital.

## References

- [1.] B.J. Bandy, D.R. Lloyd and N.V. Richardson, *Surface Sci.* **89** (1979) 344.
- [2.] F.P. Netzer, E. Bertel and J.A.D. Matthew, *Surface Sci.* **92** (1980) 43.
- [3.] S.R. Kelemen and A. Kaldor, *Chem. Phys. Lett.* **73** (1980) 205.
- [4.] M. Fleischmann, P.J. Hendra and A.J. McQuillan, *Chem. Phys. Lett.* **26** (1974) 163; D.L. Jeanmaire and R.P. Van Duyne, *J. Electroanal. Chem.* **84** (1977) 1; M.G. Albrecht and J.A. Creighton, *J. Amer. Chem. Soc.* **99**, (1977) 5215.
- [5.] R.R. Smardzewski, R.J. Colton and J.S. Murday, *Chem. Phys. Lett.* **68** (1979) 53; J.E. Rowe, C.V. Shank, D.A. Zwemer and C.A. Murray, *Phys. Rev. Lett.* **44** (1980) 1770; P.N. Sanda, J.M. Warlaumont, J.E. Demuth, J.C. Tsang, K. Christmann, and J.A. Bradley, to be published.
- [6.] J.E. Demuth, *Surf. Sci.* **69** (1977) 365.
- [7.] J.A. Simpson and C.E. Kuyatt, *Rev. Sci. Instr.* **38** (1967) 103.
- [8.] H.J. Levinstein and W.H. Robinson, *J. Appl. Phys.* **33** (1962) 3149.
- [9.] This corresponds to the guage-correction factor for benzene as supplied with our Varian ion guage.
- [10.] L. Corrsin, B. Fox and R.C. Lord, *J. Chem. Phys.* **21** (1953) 1170.
- [11.] D.J. Pouchart, *Aldrich Library of Infrared Spectra*, (Aldrich Chem. Co., Wisconsin, 1975).
- [12.] D.A. Long and E.L. Thomas, *Trans. Far. Soc.* **59**, (1963) 783.
- [13.] K. Nakamoto, *Infrared and Raman Spectra of Inorganic and Coordination Compounds*, (Wiley Interscience, NY, 1978) 211.
- [14.] E. Evans and D.L. Mills, *Phys. Rev. B* **5** (1972) 4126.
- [15.] D. Sokcevic, Z. Lenac, R. Brado and M. Sunjic. *Z. Phys. B* **28** (1977) 273.

- [16.] This assumption is borne out by the narrow variation of inclination angles we determine in analyzing close-lying pairs of vibrations (i.e.,  $\nu_{27}/\nu_{10}$  and  $\nu_{26}/\nu_{10}$ ), but is more questionable when analyzing widely-separated features. The latter may account for the large variation found for the rotational angles.
- [17.] Gas-phase electron-scattering work by I. Nenner and G.J. Schulz, J.Chem. Phys. **62**, (1975) 1747, shows strong vibrational excitations of *specifically* these two modes via temporary negative ion resonance scattering. This additional scattering contribution also explains why we see smaller than expected (dipole-derived) intensity variations with coverage for these two losses [see Fig.2].
- [18.] D.W. Turner, et al: *Molecular Photoelectron Spectroscopy*, (Wiley Interscience, NY 1970).
- [19.] W.L. Jorgensen and L. Salem, *The Organic Chemist's Book of Orbitals*, (Academic Press, NY, 1973) 263.
- [20.] W. van Niesen, G.H.F. Diercksen and L.S. Cederbaum, Chem. Phys. **10** (1975) 345.
- [21.] J.E. Demuth and D.E. Eastman, Phys Rev B **13** (1976) 1523.
- [22.] J.E. Demuth, Phys. Rev. Lett. **40** (1978) 409.
- [23.] H. Lüth, G.W. Rubloff and W.D. Grobman, Surf. Sci. **63** (1977) 325.
- [24.] We use a conventional LEED display apparatus with  $\sim 10^{-6}$  Amp. beam currents which are well recognized to disrupt, desorb or disorder weakly adsorbed molecular species. (e.g., see J.C. Tracy, J. Chem. Phys. **56** [1972] 2736.)
- [25.] H. Ibach, private communication
- [26.] J.E. Demuth and H. Ibach, Surf. Sci. **85** (1979) 365.

TABLE I. Assignment of the observed vibrations for pyridine on Ag(111)

$h_5$ -Pyridine			$d_5$ -Pyridine			Sym.	Mode No.
on Ag(111)	IR(liquid) <sup>10,11</sup>		on Ag(111)	IR(liquid) <sup>10,11</sup>			
$\nu$	$\nu$	A	$\nu$	$\nu$	A		$\nu_P^{12}$
200	- - -	- - -	(175)	- - -	- - -	B <sub>2</sub>	PM**
400	405	.55	365	371	.06	B <sub>2</sub>	27
610	605	.63	560	582	1.77	A <sub>1</sub>	10
705	700	1.39	525	530	.52	B <sub>2</sub>	26
- -	- - -	- - -	700	- - -	- - -	B <sub>2</sub>	26 + PM**
est 990	992	.99	965	962	.52	A <sub>1</sub>	9
1040	1030	1.02	1020	1006	.05	A <sub>1</sub>	8
	1068	.51	820	{ 823 }	.79	A <sub>1</sub>	7
	942	<.02		{ 823 }		B <sub>2</sub>	23
	{ 1218 }	.42	n-obs.	886	.11	A <sub>1</sub>	6
1220	{ 1218 }	.42		908	<.02	B <sub>1</sub>	16
1440	1439	1.71	1305	1301	1.77	B <sub>1</sub>	14
	1482	.71		1340	<.02	A <sub>1</sub>	5
1570	{ 1572 }	1.56	1540	{ 1542 }	1.43	B <sub>1</sub>	13
	{ 1583 }	.87		{ 1530 }	1.20	A <sub>1</sub>	4
	{ 3036 }	.41		{ 2285 }	.45*	B <sub>1</sub>	12
	{ 3036 }			2254	.68	A <sub>1</sub>	3
3040	{ 3055 }	.63	2260	{ 2293 }	.45*	A <sub>1</sub>	1
	{ 3055 }			2270	.46	A <sub>1</sub>	2
	3083	.56		2290	.45*	B <sub>1</sub>	11
n-obs.	1148	.45	n-obs.	887	.11	B <sub>1</sub>	17
n-obs.	749	1.30	n-obs.	567	<.02	B <sub>2</sub>	25

\* Overlapping bands.

\*\* Pyridine-metal-stretching frequency

### Figure Captions

- Fig.1. Vibrational loss spectra for 0.4 L (solid line) and 0.8 L (dotted line) exposures of  $d_5$ -pyridine to Ag(111). (The dashed line under the 0.6 L exposure spectra shows the spectrometer background signal at these magnifications). The IR-absorbances are compared to the loss spectra where we have shown all absorbances within 1% of the largest value [10,11]. (The absorbances denoted by \* have been reduced by 1/3).
- Fig.2. Vibrational loss spectra for pyridine between 350-1500  $\text{cm}^{-1}$  as a function of exposure. The spectra shown at  $2 \times 10^{-7}$  Torr ambient pressures of pyridine corresponds to the onset of condensation, and the formation of the first physisorbed layer.
- Fig.3. UV Photoemission difference spectra ( $h\nu=21.2$  eV)(a) between the clean Ag(111) surface and a 0.35 L exposure to pyridine (the  $\pi$ -bonded phase) and (b) between a 0.52 L and 1.0 L exposure to pyridine (the nitrogen lone-pair bonded phase). A high exposure spectra for condensed (randomized) pyridine is shown in (c) which is compared to the gas phase ionization spectra [18]. All gaseous ionization features are derived from single orbitals except the second lowest feature which is derived from two orbitals [20].
- Fig.4. Schematic diagram of the orientation and bonding of (a) the low coverage ( $< 0.4$  L exposure) phase and (b) the high coverage ( $> 0.5$  L exposure) compressional phase. Discrete bonding sites for pyridine on Ag(111) as well as pyridine's hydrogen atoms are not shown. In (b), the two molecules shown lie slightly below (right) and above (left) the plane of the page.

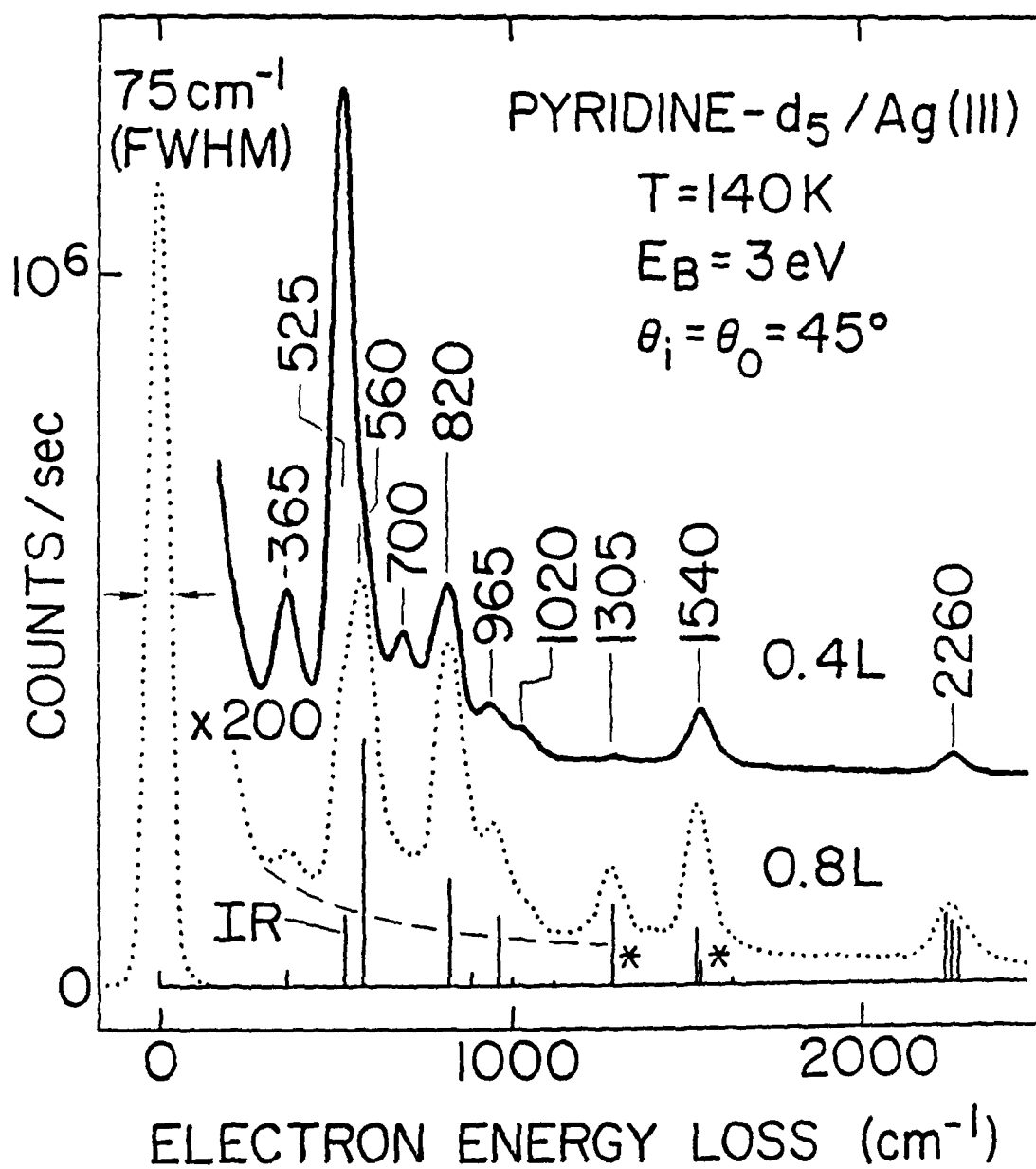


FIG 1  
DEMUTH



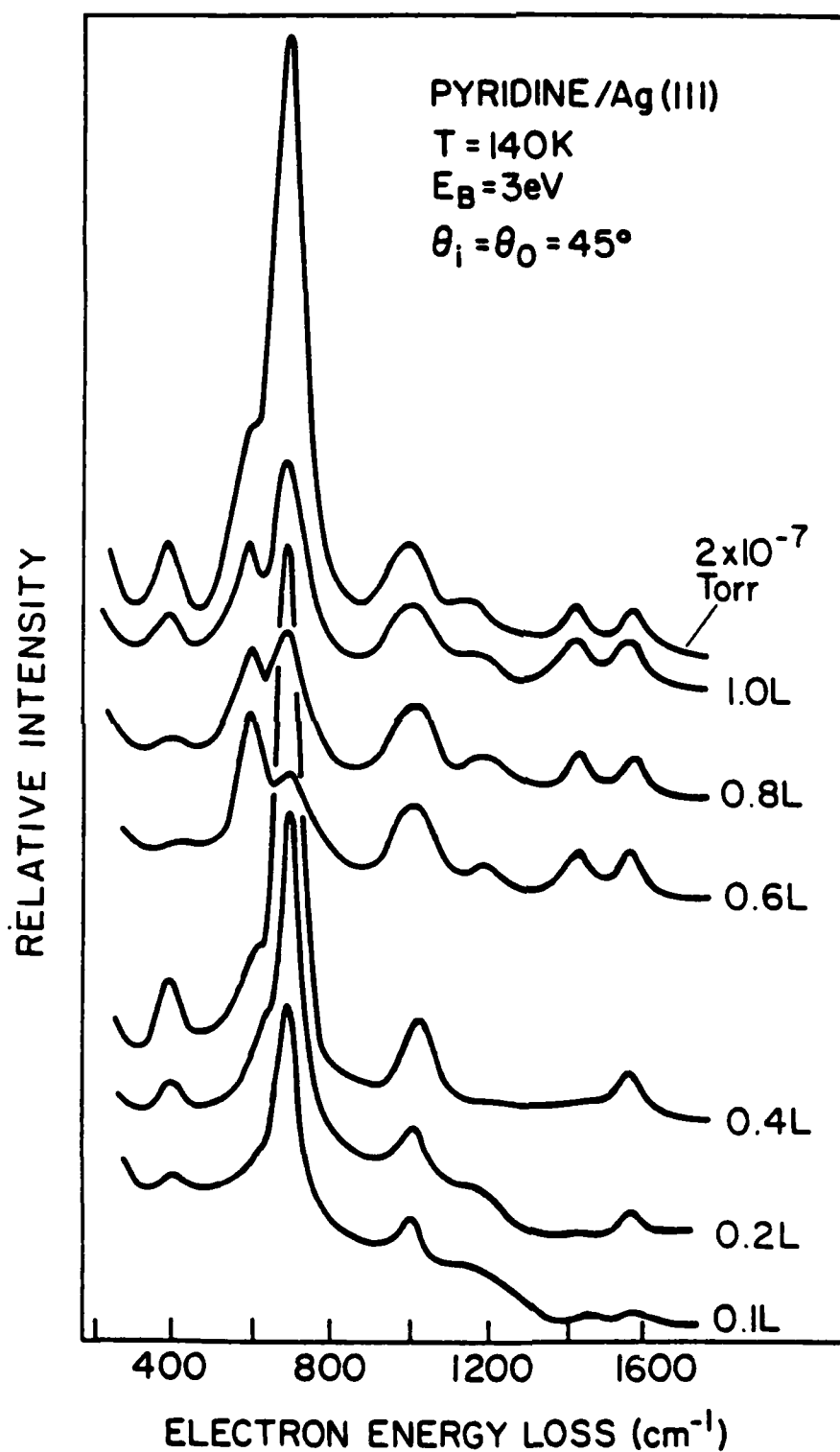


FIG 2

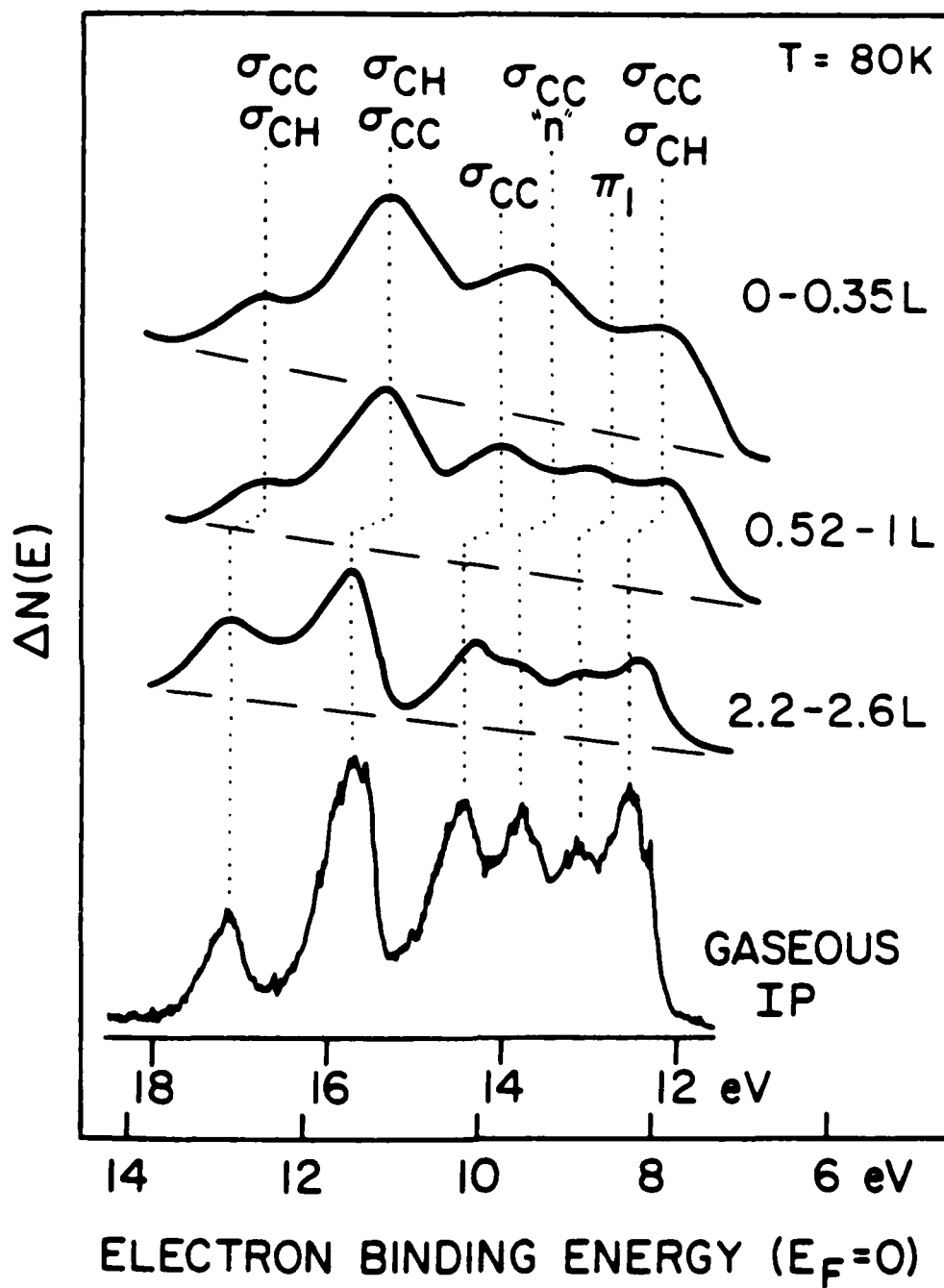
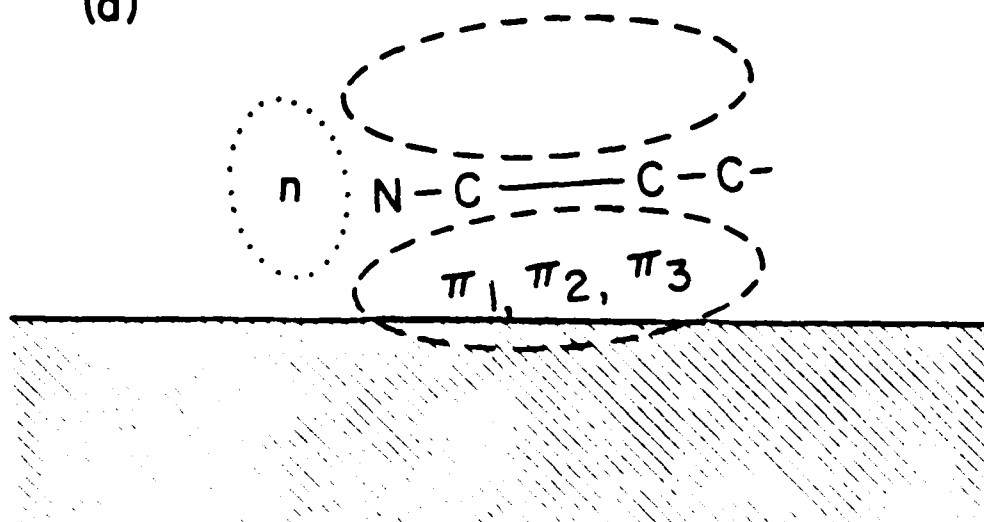
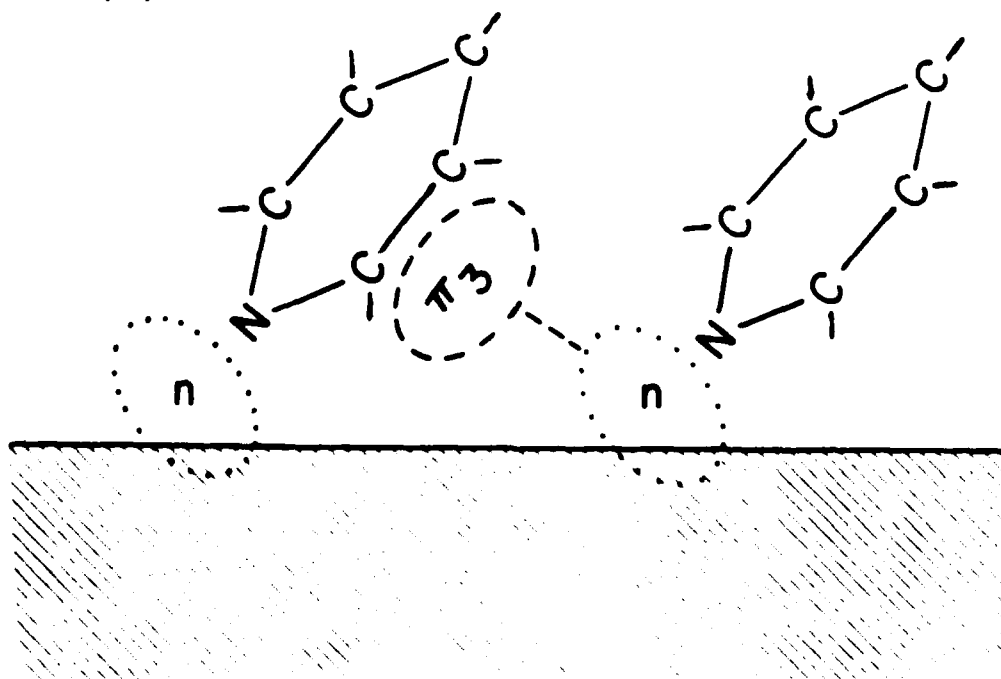


FIG 3

(a)



(b)



TECHNICAL REPORT DISTRIBUTION LIST, GEN

	<u>No. Copies</u>		<u>No. Copies</u>
Office of Naval Research Attn: Code 472 800 North Quincy Street Arlington, Virginia 22217	2	U.S. Army Research Office Attn: CRD-AA-IP P.O. Box 1211 Research Triangle Park, N.C. 27709	1
ONR Branch Office Attn: Dr. George Sandoz 536 S. Clark Street Chicago, Illinois 60605	1	Naval Ocean Systems Center Attn: Mr. Joe McCartney San Diego, California 92152	1
ONR Area Office Attn: Scientific Dept. 715 Broadway New York, New York 10003	1	Naval Weapons Center Attn: Dr. A. B. Amster, Chemistry Division China Lake, California 93555	1
ONR Western Regional Office 1030 East Green Street Pasadena, California 91106	1	Naval Civil Engineering Laboratory Attn: Dr. R. W. Drisko Port Hueneme, California 93401	1
ONR Eastern/Central Regional Office Attn: Dr. L. H. Peebles Building 114, Section D 666 Summer Street Boston, Massachusetts 02210	1	Department of Physics & Chemistry Naval Postgraduate School Monterey, California 93940	1
Director, Naval Research Laboratory Attn: Code 6100 Washington, D.C. 20390	1	Dr. A. L. Slafkosky Scientific Advisor Commandant of the Marine Corps (Code RD-1) Washington, D.C. 20380	1
The Assistant Secretary of the Navy (RE&S) Department of the Navy Room 4E736, Pentagon Washington, D.C. 20350	1	Office of Naval Research Attn: Dr. Richard S. Miller 800 N. Quincy Street Arlington, Virginia 22217	1
Commander, Naval Air Systems Command Attn: Code 310C (H. Rosenwasser) Department of the Navy Washington, D.C. 20360	1	Naval Ship Research and Development Center Attn: Dr. G. Bosmajian, Applied Chemistry Division Annapolis, Maryland 21401	1
Defense Technical Information Center Building 5, Cameron Station Alexandria, Virginia 22314	12	Naval Ocean Systems Center Attn: Dr. S. Yamamoto, Marine Sciences Division San Diego, California 91232	1
Dr. Fred Saalfeld Chemistry Division, Code 6100 Naval Research Laboratory Washington, D.C. 20375	1	Mr. John Boyle Materials Branch Naval Ship Engineering Center Philadelphia, Pennsylvania 19112	1

TECHNICAL REPORT DISTRIBUTION LIST, GENNo.  
Copies

Dr. Rudolph J. Marcus  
Office of Naval Research  
Scientific Liaison Group  
American Embassy  
APO San Francisco 96503

1

Mr. James Kelley  
DTNSRDC Code 2803  
Annapolis, Maryland 21402

1

TECHNICAL REPORT DISTRIBUTION LIST, 056

	<u>No. Copies</u>		<u>No. Copies</u>
Dr. D. A. Vroom IRT P.O. Box 80817 San Diego, California 92138	1	Dr. C. P. Flynn Department of Physics University of Illinois Urbana, Illinois 61801	1
Dr. G. A. Somorjai Department of Chemistry University of California Berkeley, California 94720	1	Dr. W. Kohn Department of Physics University of California (San Diego) LaJolla, California 92037	1
Dr. L. N. Jarvis Surface Chemistry Division 4555 Overlook Avenue, S.W. Washington, D.C. 20375	1	Dr. R. L. Park Director, Center of Materials Research University of Maryland College Park, Maryland 20742	1
Dr. J. B. Hudson Materials Division Rensselaer Polytechnic Institute Troy, New York 12181	1	Dr. W. T. Peria Electrical Engineering Department University of Minnesota Minneapolis, Minnesota 55455	1
Dr. John T. Yates Surface Chemistry Section National Bureau of Standards Department of Commerce Washington, D.C. 20234	1	Dr. Narkis Tzoar City University of New York Convent Avenue at 138th Street New York, New York 10031	1
Dr. Theodore E. Madey Surface Chemistry Section Department of Commerce National Bureau of Standards Washington, D.C. 20234	1	Dr. Chia-wei Woo Department of Physics Northwestern University Evanston, Illinois 60201	1
Dr. J. M. White Department of Chemistry University of Texas Austin, Texas 78712	1	Dr. D. C. Mattis Polytechnic Institute of New York 333 Jay Street Brooklyn, New York 11201	1
Dr. Keith M. Johnson Department of Metallurgy and Materials Science Massachusetts Institute of Technology Cambridge, Massachusetts 02139	1	Dr. Robert M. Hexter Department of Chemistry University of Minnesota Minneapolis, Minnesota 55455	1
<del>Dr. J. E. Demuth IBM Corporation Thomas J. Watson Research Center P.O. Box 218 Yorktown Heights, New York 10593</del>	<del>1</del>	Dr. R. P. Van Duyne Chemistry Department Northwestern University Evanston, Illinois 60201	1

TECHNICAL REPORT DISTRIBUTION LIST, 056

	<u>No.</u> <u>Copies</u>		<u>No.</u> <u>Copies</u>
Dr. M. G. Lagally Department of Metallurgical and Mining Engineering University of Wisconsin Madison, Wisconsin 53706	1	Dr. J. Osteryoung Chemistry Department SUNY, Buffalo Buffalo, New York 14214	1
Dr. Robert Gomer Department of Chemistry James Franck Institute 5640 Ellis Avenue Chicago, Illinois 60637	1	Dr. G. Rubloff I.B.M. Thomas J. Watson Research Center P. O. Box 218 Yorktown Heights, New York 10598	1
Dr. R. G. Wallis Department of Physics University of California, Irvine Irvine, California 92664	1	Dr. J. A. Gardner Department of Physics Oregon State University Corvallis, Oregon 97331	1
Dr. D. Ramaker Chemistry Department George Washington University Washington, D.C. 20052	1	Dr. G. D. Stein Mechanical Engineering Department Northwestern University Evanston, Illinois 60201	1
Dr. P. Hansma Chemistry Department University of California, Santa Barbara Santa Barbara, California 93106	1	Dr. K. G. Spears Chemistry Department Northwestern University Evanston, Illinois 60201	1
Dr. P. Hendra Chemistry Department Southampton University England SO9JNH	1	Dr. R. W. Plummer University of Pennsylvania Department of Physics Philadelphia, Pennsylvania 19104	1
Professor P. Skell Chemistry Department Pennsylvania State University University Park, Pennsylvania 16802	1	Dr. E. Yeager Department of Chemistry Case Western Reserve University Cleveland, Ohio 41106	2
Dr. J. C. Hemminger Chemistry Department University of California, Irvine Irvine, California 92717	1	Professor George H. Morrison Cornell University Department of Chemistry Ithaca, New York 14853	1
Dr. Martin Fleischmann Department of Chemistry Southampton University Southampton SO9 5NH Hampshire, England	1	Professor N. Winograd Pennsylvania State University Chemistry Department University Park, Pennsylvania 16802	1
		Professor Thomas F. George The University of Rochester Chemistry Department Rochester, New York 14627	1